Journal of Alloys and Compounds 769 (2018) 1080–1087

Contents lists available at ScienceDirect

Journal of Alloys and Compounds

journal homepage: http://www.elsevier.com/locate/jalcom

# Effect of SiC particle size and heat-treatment on microhardness and corrosion resistance of NiP electrodeposited coatings

D. Ahmadkhaniha [a, *], F. Eriksson [b], P. Leisner [a, c], C. Zanella [a]

[a] School of Engineering, Jönköping University, P.O. Box 1026, Gjuterigatan 5, SE-551 11, Jönköping, Sweden
[b] Department of Physics, Chemistry and Biology (IFM), Linköping University, 581 83, Linköping, Sweden
[c] RISE Research Institute of Sweden, P.O. Box 857, Brinellgatan 4, SE-501 15, Borås, Sweden

ARTICLE INFO

*Article history:*
Received 23 May 2018
Received in revised form
1 August 2018
Accepted 2 August 2018
Available online 4 August 2018

*Keywords:*
Electrodeposition
NiP
SiC
Microhardness
Polarization
Heat-treatment

ABSTRACT

Electrodeposition of NiP composite coatings with nano and sub-micron sized SiC has been carried out to investigate the possibility of replacing hard chromium coatings. The composition and structure of the coatings were evaluated by energy dispersive X-ray spectroscopy (EDS) and X-ray diffraction (XRD) analysis, respectively. Microhardness was measured by Vickers indentation and polarization measurements were carried out to study the corrosion behavior of the coatings. The results showed that submicron particles can be codeposited with a higher content as compared to nano sized ones. However, even if a smaller amount of the nano-sized SiC particles are incorporated in the coating, the contribution to an increasing microhardness was comparable with the submicron sized particles, which can be related to the higher density of codeposited particles. SiC particles did not change the anodic polarization behavior of NiP coatings in a 3.5% NaCl solution. Finally, the effect of heat-treatment on the coatings properties at 400 °C for 1 h was studied to investigate the contribution of particles and heat-treatment on hardness and corrosion properties. It was found that the heat-treatment doubled the microhardness and changed the anodic polarization behavior of the coatings from passive to active with respect to the as-plated conditions.



## 1. Introduction

The electroplating industry in Europe is undergoing changes due to environmental concerns. Hard chromium plating using hexavalent Cr, which has wide industrial applications [1], has been restricted by the European Union due to environmental issues. Therefore, substitute coating materials and new designs have been under study. Alternative processes which are free of hexavalent chromium should provide the requested properties including high hardness, low friction coefficient, and excellent wear and corrosion resistance [2].

In this regard, Ni-based alloys, such as e.g. nickel–tungsten (Ni-W) coatings [3,4] NiP and NiB [2,5–8], can be suitable candidates due to their high hardness and good corrosion resistance as well as the chance of hardening by heat-treatment. NiP coatings have attracted a lot of attentions among the researchers recently. The properties of NiP coatings depend on their phosphorus content. High phosphorus (P>10%wt) alloys are amorphous and in the as-plated state they are characterized by remarkable corrosion resistance, although with lower microhardness and wear resistance compared to low phosphorus containing NiP coatings [9,10].

The microhardness of Ni high P can be further increased by heat-treatment and reach values comparable to those of hard Cr coatings. Heat-treatment at temperatures between 300 and 400 °C can improved the microhardness of NiP coatings [11], whereas, may not always be applicable due to the substrate sensitivity to elevated temperatures. Furthermore, heat-treatment can introduce micro-cracks in the coating which reduce the corrosion protection. Incorporation of hard ceramic particles in the coating could be an alternative to heat-treatment as the hardening mechanism [12]. Several researchers have successfully codeposited WC, SiC, $Si_3N_4$ in Ni-P matrices [12–16]. Malfatti et al. [17] studied the effect of SiC addition on the corrosion behavior of NiP/SiC coatings. Garcia et al. [18] observed an improvement in corrosion resistance by the addition of SiC particles to a pure Ni matrix, while Zanella et al. [19] observed a minor increase in polarization current of Ni coatings by addition of micron sized SiC particles. Aslanyan et al. [20] showed that wear loss of NiP coatings was reduced by addition SiC particles,

* Corresponding author.
*E-mail address:* donya.ahmadkhaniha@ju.se (D. Ahmadkhaniha).

https://doi.org/10.1016/j.jallcom.2018.08.013
0925-8388/

however, heat-treated NiP/SiC coatings had higher wear loss than pure NiP. According to Araghi et al. [21], addition of $B_4C$ to a NiP matrix, increases hardness to 1200 MPa while the corrosion resistance decreases. It was also reported by Shafiee et al. [22] that nanocomposite modulated multilayer coatings (Ni/Ni-$Al_2O_3$) can be a possible alternative to single layer nanocomposite coatings in tribological applications. Multilayer Ni–W and Ni–W-$Al_2O_3$ coatings were exhibited as a proper candidate for corrosion and wear resistant coatings [23]. However, increasing tungsten in the Ni–W coatings which improves wear resistance, can increase possibility of surface cracking and lead to poor corrosion resistance. To overcome this problem, functionally graded (FG) nanocomposite Ni–W–$Al_2O_3$ coating was produced by Allahyarzadeh et al. [24,25]. They designed the coating structure in a way to have more nickel content in the vicinity of the substrate/coating interface, and the highest content of tungsten and alumina in the outermost layer which reduced the possibility of the crack initiation and increased wear resistance. Lei et al. [26] also observed an improvement in wear resistance and microhardness of FG Ni-W/BN(h) coatings respect to that of uniform Ni-W/BN(h) coatings. Beltowska-Lehman et al. [27] also developed conditions for producing homogeneous and crack free NiW/$ZrO_2$ coatings. The graded Ni–P coatings with the design of low P/medium P/high P layers from the substrate to the surface had the best wear resistance as was shown by Hadipour et al. [28].

According to the above information, micron-sized ceramic particles in the coatings can improve the hardness and wear but may also introduce defects such as voids at the particle–matrix interface which might reduce the corrosion resistance of such systems. Moreover, in the case of wear, micro particles can be released and behave as a third body in the wear system, accelerating the wear rate. These challenges may be overcome, by the use of nanoparticles [19]. In addition, Lekka et al. [29] observed the reduction in corrosion resistance of pure Ni coatings by incorporation of micro-SiC particles, whereas, the nanocomposites exhibited the highest corrosion resistance due to the more compact and fine-grained microstructure. As a result, this study was carried out to compare the effect of the particles size on microhardness and corrosion resistance of NiP coating. Although different ceramic particles have been investigated by researchers, Aslanyan et al. [20] reported that incorporation of SiC particles in a Ni-P matrix is the most effective combination of reducing cost and improving performance in industrial applications. As indicated, plenty of work has been done on Ni based composite coatings. Most of the papers relate to Ni coatings or different Ni alloys, so it is important to fill the lack of electroplated NiP alloys. Moreover, a lot of papers compare micro and nano powders, finding that micro particles are more effective in hardening and nano ones are better for corrosion protection. In this study, an intermediate size of particles will be proposed to compromise as well. Therefore, in this study, SiC particles with 50, 100 and 500 nm in size were chosen as reinforcing particles and their effects on hardness and corrosion resistance of Ni high P coatings were studied.

## 2. Materials and methods

### 2.1. Sample preparation and deposition

Nickel high phosphorous alloys, hereafter referred to as NiP, were electro-deposited using a modified Watts bath (in a circular cell of 2 l) on substrates of low carbon steel and brass panels with area of 25 $cm^2$. Prior to deposition the steel substrates were mechanically ground with SiC grades #500 and #800, and ultrasonically cleaned in an alkaline soap and activated by pickling for 8 min in 2.5 M $H_2SO_4$. Between each step the substrate was rinsed by distilled water. Brass substrates were ready to plate substrates without any pre-treatment and they assured the best adhesion to the substrate; hence, they were used for the as-plated conditions. While steel substrates were used for heat-treated condition and the corrosion tests.

In the modified Watts bath the electrodes were positioned vertically and parallel at a distance of 12 cm from each other. The composition of the plating bath was updated from bath in Ref. [30] which contains $NiSO_4{\cdot}7H_2O$, $NiCl_2{\cdot}6H_2O$, $H_3PO_3$, $H_3BO_3$ and two additives (saccharin and sodium dodecyl sulfate). The ratio of $Ni^{2+}$/$PO_3^{3-}$ was 3.25 and pH of the bath was adjusted to 2.15 before each plating by adding sulfuric acid or sodium hydroxide. To produce composite coatings 20 g $l^{-1}$ of silicon carbide particles (β-SiC, provided by Get Nano Materials) with average size of 50 nm, 100 nm, and 500 nm, were added in the bath, which was stirred for 24 h before plating as well as during plating. Deposition was carried out at 4 A/$dm^2$ at 70 °C and the bath was agitated by magnetic stirrer at 250 rpm. The current efficiency was calculated by measuring the weight of the coating and comparing to the theoretical deposited mass, and it was around 50%. To determine the weight of the coating (Δm) in each plating, substrates were weighted before plating and after plating by a scale with 0,0001 accuracy. The Faraday law (Eq. (1)) was used to calculate the theoretical mass ($m_t$) of the coating during deposition and finally current efficiency was calculated according to Eq. (2).

$$m_t = \left(\frac{M_1}{N_1} + \frac{M_2}{N_2}\right) \times \frac{It}{F} \quad (1)$$

$$\text{Current efficiency } \% = \frac{\Delta m}{m_t} \times 100 \quad (2)$$

where, $M_1$ and $M_2$ are the molar mass of the Ni and P, respectively. $N_1$ and $N_2$ are the oxidation state of the Ni and P, respectively, I is the applied current (A), t is the total time of deposition (s) and F is the Faraday's constant (96,485 coulombs) [31].

In order to investigate the effect of heat-treatment on the microhardness of the coatings, some of the samples were annealed at 400 °C with heating rate of 10 °C/min for 1 h in air and in a controlled Argon atmosphere.

### 2.2. Characterizations

Morphology and composition of the coatings were investigated by means of scanning electron microscopy (SEM, JEOL 7001F) equipped with energy dispersive X-ray spectroscopy (EDS, EDAX). Surface roughness of the coatings was measured by surface profilometer (Surtronic 3+). The cross section of heat-treated samples was also observed by SEM after etching in a solution of 50% $HNO_3$ and 30% $CH_3COOH$ for 10 s. X-ray diffraction was performed using a Panalytical X'Pert diffractometer giving Cu-Kα X-rays (λ = 1.54 Å) to investigate the structure of the coatings. Phase transformations were studied by differential scanning calorimetry (DSC, Netzsch 404C) at a heating rate of 10 °C/min in the temperature range 25–550 °C using Argon as protective media. The microhardness of the coatings was measured by Vickers indentation (NanoTest™ Vantage) with an indentation load and dwell time of 100 mN and 10 s, respectively. To measure the microhardness, the samples were cross-sectioned and mechanically polished. 15 measurements were performed on 2 different samples with the same condition to estimate the average values. The electrochemical behavior of the coatings was studied by a potentiodynamic polarization technique in a 3.5% NaCl aqueous solution at room temperature. Ag/AgCl (3 M KCl, 0.21 vs. SHE/V) and platinum electrodes were used as the

reference and counter electrodes, respectively. The coatings with exposed area of 1 $cm^2$ was selected as working electrode. The anodic potentiodynamic polarization was performed after 20 min delay in the potential range −50 mV to 1000 mV respect to the open circuit potential (OCP) with a scan rate of 0.2 mV/s. The tests were repeated at least twice on different specimens of the same coating.

## 3. Results and discussion

### 3.1. Morphology and composition

SEM micrographs related to the surface of the coatings are observed in Fig. 1. It can be seen that as-plated NiP (Fig. 1a) and NiP/SiC coatings (Fig. 1b–d) have a nodular morphology. The small dark gray areas in the SEM images in Fig. 1 are related to pores on the surface of the coatings and the small white areas on top of the coatings are due to the charging of insulating SiC particles. EDS map of NiP/SiC100 nm (comparing Fig. 2a and b) also confirms that small white areas are SiC particles.

By comparing Fig. 1b–d it can be concluded that smaller SiC particles (50 nm) resulted in finer nodular morphology respect to the larger particles, and in the case of sub-micron SiC particles (500 nm), the nodularity decreased which was also observed by Sarret et al. [32]. Surface roughness and nodular diameter in NiP and composite coatings were measured and the results were listed in Table 1. According to Table 1, surface roughness increased by addition SiC100 and 500 nm. However, SiC particles did not affect remarkably the nodular size. Although, SiC50 nm decreased the size of nodular slightly, by increasing the size of the SiC particles, the nodular diameter increased.

EDS analysis (Fig. 3a) shows that the phosphorous content of the metallic coatings is around 16 wt% and is independent of particles codeposition. In Fig. 3b, it is seen that the highest amount of SiC, about 8 vol%, was incorporated when using 500 nm SiC particles. On the other hand, SiC particle density is higher when using 50 nm-sized particles. To measure particle density, first vol% of SiC was calculated by considering 7.75 and 3.21 $g/cm^3$ as density of NiP matrix and SiC particles, respectively. Then SiC particle density which is the number of the particles per $cm^3$ was measured by considering spherical shape for SiC particles.

### 3.2. Structure

XRD patterns of NiP and composite coatings are shown in Fig. 4a. These are characteristic of coatings with a high fraction of an amorphous phase. The broad diffraction peak centered around $2\Theta = 44.6^\circ$ corresponds to some nanocrystalline Ni domains in an amorphous phase. Alloying with P results in distortion of the base Ni lattices due to the atomic size difference. XRD analysis determined the lattice parameter of the NiP coatings in this study as 3.69 Å while the lattice parameter for Ni is 3.52 Å. With increasing P content, the lattice distortion becomes larger and finally an amorphous phase is formed. The effect of phosphorus content on crystallinity of NiP coating has been addressed also by other researchers [13,33–35]. The peaks at $2\Theta = 72^\circ, 87^\circ, 130^\circ$ and $137^\circ$ are related to the substrate. According to Fig. 3a, the addition of SiC particles does not affect the structure of NiP coatings while Shakoor et al. [5] showed that the addition of $Al_2O_3$ particles can induce crystallization in NiB coatings.

The heat-treatment leads to crystallization, as evidenced by the sharp diffraction peaks, and the precipitation of a second phase (Fig. 4b). Phase analysis of the NiP coatings after heat-treatment identified that the coating consists of Ni and $Ni_3P$ phases. The diffraction peaks at $2\Theta = 44.6^\circ$, 51.8 and $75.6^\circ$ originate from diffraction of Ni and the others are related to $Ni_3P$. Composite coatings demonstrate similar structure to NiP ones after heat-treatment. Since all reflections of the phases appeared in the diffraction pattern, with intensity ratios in agreement with those given for the pdf reference pattern (pdf-no 01-074-1384), it is concluded that it is polycrystalline with randomly oriented

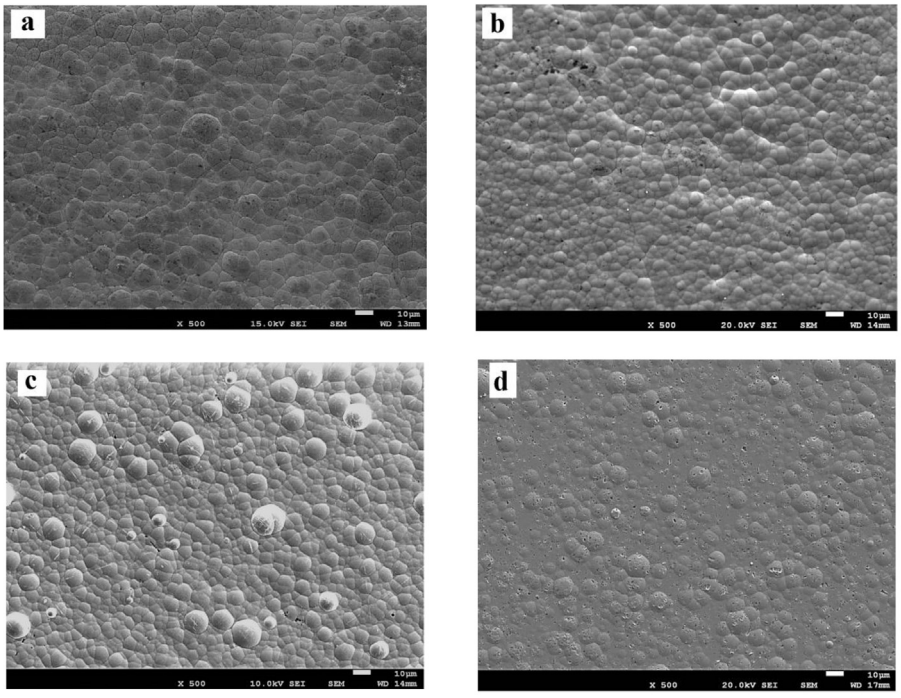


**Fig. 1.** SEM micrographs of the surface of (a) NiP, (b) NiP/SiC50 nm, (c) NiP/SiC100 nm, (d) NiP/SiC500 nm.

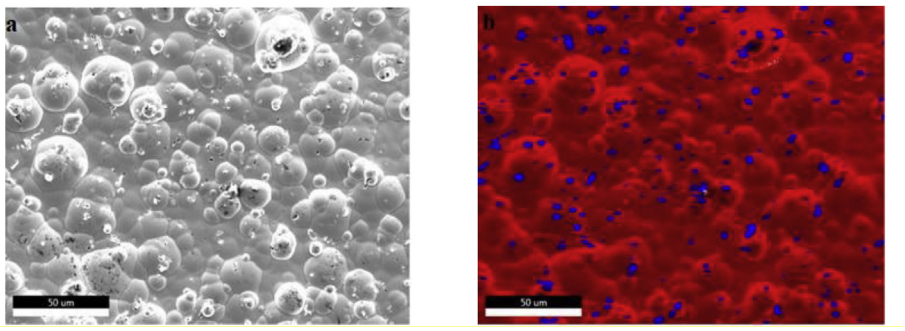


**Fig. 2.** (a) SEM image and (b) EDS map of Si on the surface of NiP/SiC100 nm. Blue color is the indicator of Si. (For interpretation of the references to color in this figure legend, the reader is referred to the Web version of this article.)

**Table 1**
$R_a$ (μm) values and mean nodular diameters (μm) of NiP and composite coatings.

| Coatings | NiP | NiP/SiC50 nm | NiP/SiC100 nm | NiP/SiC500 nm |
|---|---|---|---|---|
| $R_a$ | 0.35 ± 0.06 | 0.36 ± 0.12 | 0.56 ± 0.23 | 1.22 ± 0.55 |
| Mean nodular diameter | 6.9 ± 2.6 | 6.0 ± 1.6 | 6.1 ± 2.5 | 7.3 ± 2.2 |

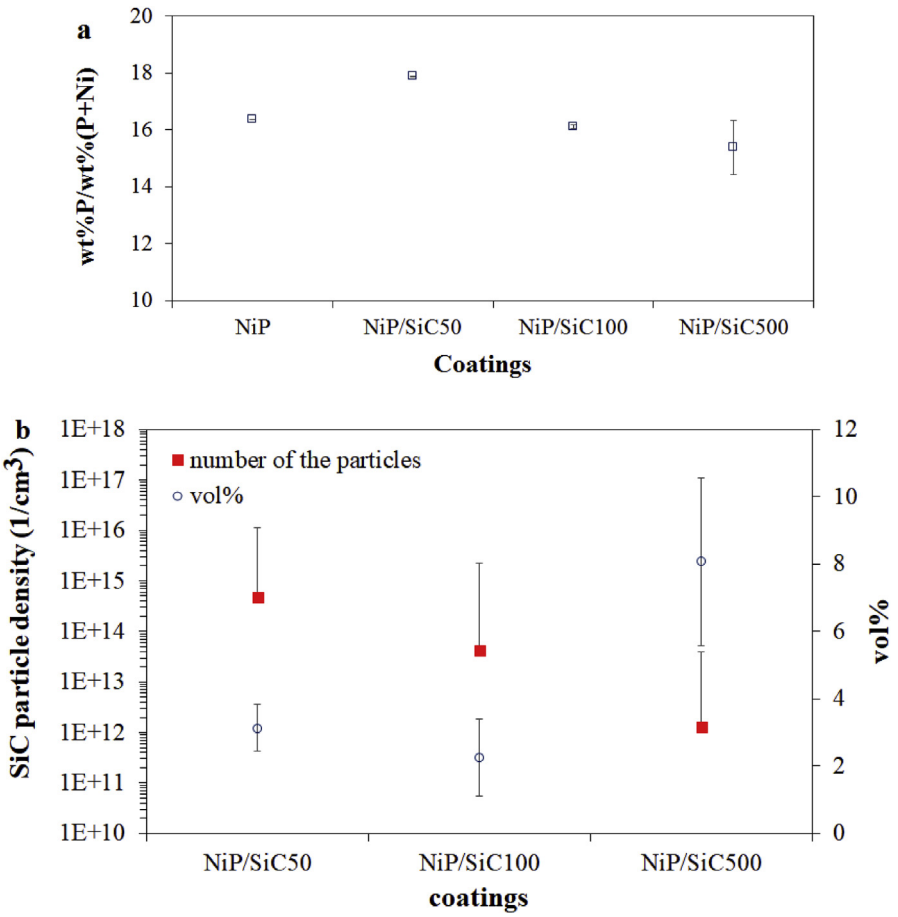


**Fig. 3.** (a) Ratio of wt%P/wt%(Ni+P), (b) SiC particle density and vol% of codeposited SiC particles in the coatings.

crystallites in all directions. Furthermore, there is a peak shift towards lower angles when adding SiC particles with smaller particle size. This could be due to the higher particle density which can influence strain in the coatings as well.

### 3.3. DSC

Coating's phase transformation was studied by DSC and the results are presented in Fig. 5. For a clear comparison, the DSC scan of steel substrate is also shown. There is no phase transformation in

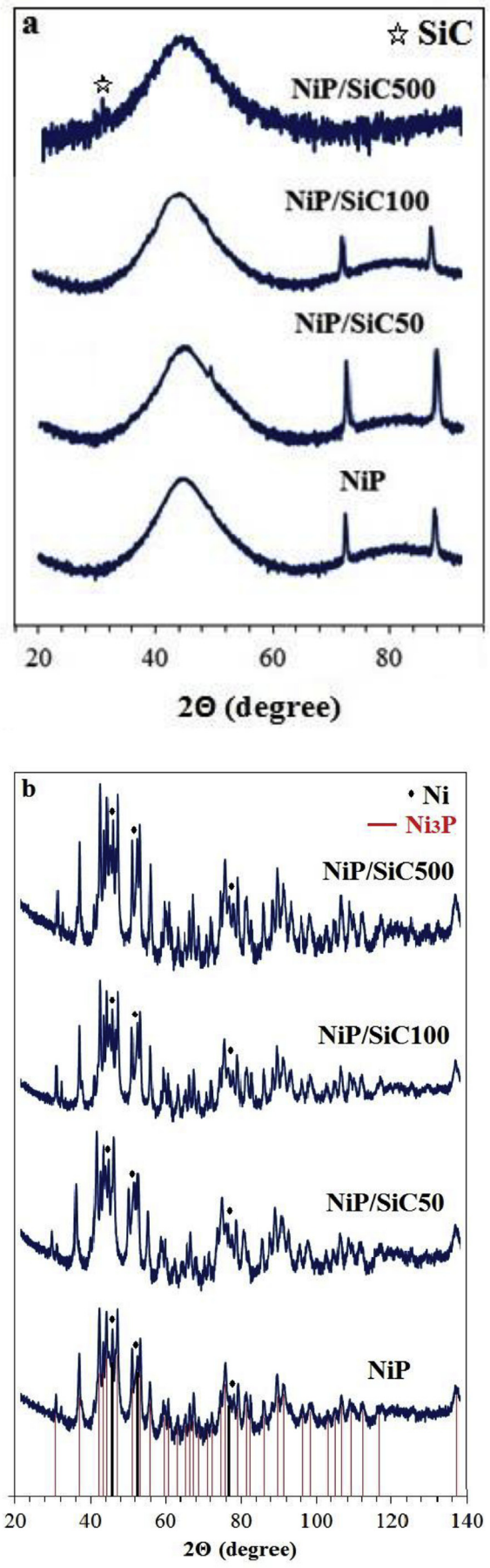


**Fig. 4.** XRD patterns of NiP and composite coatings in (a) as-plated and (b) heat-treated for 1 h at 400 °C.

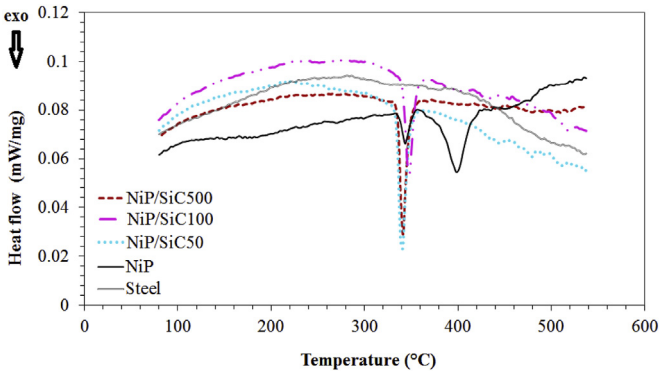


**Fig. 5.** DSC scans of NiP and composite coatings.

the substrate (steel) in the entire studied range of temperature. The NiP coating exhibits two exothermic peaks at 343 and 398 °C which correspond to the crystallization of fcc Ni and nucleation of bct $Ni_3P$ precipitation. However, NiP/SiC50, 100 and 500 nm composite coatings demonstrate an exothermic peak at 341, 348, and 341 °C, respectively. It has been reported that the phase transformation temperature depends on the phosphorus contents of the coating [36], whereas, in this study the P content of all coatings is equal (Fig. 3a), therefore, there is no significant difference in precipitation temperature of $Ni_3P$ between NiP and composite coatings. Dhanapal et al. [31] and Taheri [36] attributed the peak at 340 °C to crystallization of fcc nickel and the peak at 395 °C (observed by Dhanapal et al. [31]) or 348 °C (observed by Taheri [36]) to precipitation of $Ni_3P$ phase. In this study, in composite coatings, only a single peak is observed clearly which discloses that the crystallization of Ni and precipitation of $Ni_3P$ happened simultaneously. This was also reported by Balaraju et al. [37] although at a temperature of 340 °C.

It should be noted that the size of the particles did not influence the phase transformation temperature while Jiaqiang et al. [38] have found that the nanometric $Al_2O_3$ particles reduced the crystallization temperature of Ni-P-$Al_2O_3$ coatings and according to Balaraju et al. [39] study, there was a slight increase in crystallization temperature (around 20 °C) with the incorporation of $Si_3N_4$ particles to NiP coatings.

### 3.4. Microhardness

The microhardness of the coatings was measured on the cross section of the coatings and the results are shown in Fig. 6. As it is observed the microhardness of as-plated NiP coating is around $630 \pm 81 HV_{0.01}$ and by addition of ceramic particles the microhardness increased up to $720 \pm 66$ $HV_{0.01}$ for NiP/SiC500 nm. The difference in the microhardness values of the composite coatings is not linearly proportional to the SiC content, which can be due to agglomeration of particles. Chou et al. [40] also reported that SiC particles did not cause strong dispersion hardening.

It seems that the size of the particle or particle density affects the microhardness as well as their vol%. Higher vol% decreases or hinders the plastic deformation of the matrix while smaller particles may pin the grain boundaries and dislocations when has higher density. Garcia et al. [41] thought that the properties of the coatings can be affected by the density of the ceramic particles more than their vol%. Wasekar et al. [42] demonstrated that there is a critical amount for vol% of SiC particles in NiW matrix above which, hardness of the coating decreases. This can be attributed to the sharp increase in triple junction volume fraction and weak interface bonding of the particles and matrix. Meanwhile, higher vol% of SiC

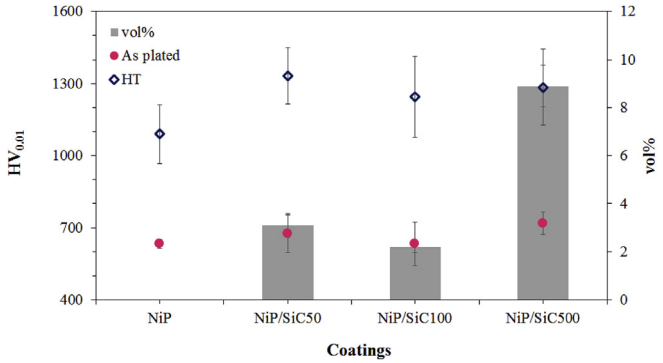


**Fig. 6.** Microhardness of as-plated and heat-treated NiP and composite coatings.

might result in finer structure which causes Hall-Petch breakdown. However, in this study, the maximum microhardness value in as-plated condition was obtained by NiP/SiC500 nm which has the highest vol% in the coating.

The microhardness of NiP coating is further increased up to 1100 ± 122 $HV_{0.01}$ (Fig. 6) by heat-treatment at 400 °C for 1 h owing to the crystallization of amorphous phase of NiP matrix and precipitation of hard $Ni_3P$ phase based on XRD patterns (Fig. 4b). It is well known that dissimilar phase boundaries are more effective in suppressing dislocation movement due to greater strain incompatibility and higher density of geometrically necessary dislocations [43]. The volumetric shrinkage due to the crystallization of the nickel and precipitation of phosphide phase can cause internal stress and cracks which influence the microhardness values. Furthermore, Chang et al. [44] explained that relaxation of non-equilibrium grain boundaries in as-plated conditions during annealing brings obstacles and difficulties for dislocation movements. There was also an argument that all phosphorus content does not precipitate as $Ni_3P$ and there is some segregation of P at the grain boundaries which can contribute in strengthening as well. However, this hypothesis was refused by Zimmerman et al. [45] since their transmission electron microscopy study showed no difference in phosphorus content in the grains and in the grain boundaries. It should be considered that they studied a Ni-5wt.%P coating that was annealed at 400 °C, hence, there has not been

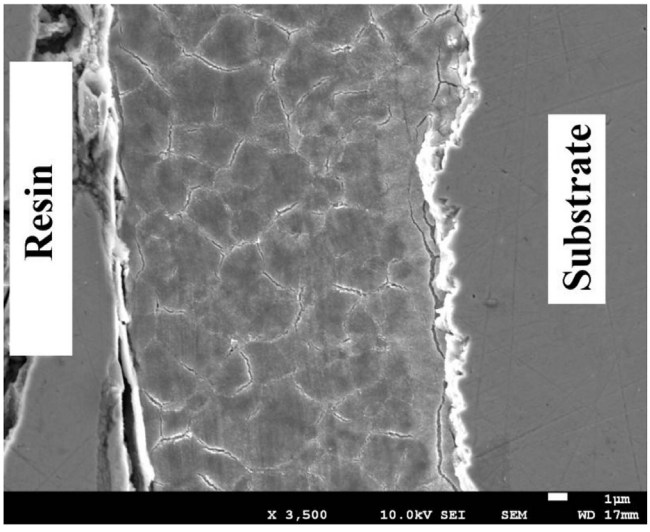


**Fig. 7.** Cross sectional SEM image of heat-treated NiP/SiC500 nm.

any established data for high phosphorus coatings yet. Grain boundary segregation and chemical ordering transitions were also observed in nanocrystalline Ni-W alloys with increasing annealing temperature [4].

According to Fig. 6, composite coatings have a higher microhardness with respect to NiP after heat-treatment, while in the as-plated condition their microhardness values (except NiP/SiC500) were comparable. This might be related to the lower grain size of composite coatings due to pining grain boundaries by SiC particles. It should also be noted that after heat-treatment, despite the different vol% of SiC, the microhardness of the composite coatings is comparable. This can be attributed to the higher amount of microcracks in NiP/SiC500 nm, as shown in the cross section of heat-treated NiP/SiC500 nm coating after etching in Fig. 7.

According to this study, the maximum microhardness value of NiP and composite coatings in as-plated condition was about 700 $HV_{0.01}$ while for hard chromium electroplated one is between 800 and 1000 HV as seen by Amoush et al. [46], Saghi Beyragh et al. [47] and Sohi et al. [48]. However, after heat-treatment, microhardness of NiP and NiP composite coatings exceeded the microhardness values of hard chromium one.

### 3.5. Electrochemical behavior

The electrochemical behavior of the coatings was evaluated by polarization in 3.5% NaCl solution at room temperature. Anodic polarization behavior was measured on 1 $cm^2$ of the sample. Fig. 8a shows that all coatings (NiP and composite ones) have the same anodic polarization behavior and demonstrate a passive behavior in the as-plated condition, therefore, particles are not hindering the passive oxide formation or stability.

$I_{corr}$ and $E_{corr}$ of the coatings are listed in Table 2. According to Table 2, composite coatings except NiP/SiC500, have a bit higher corrosion rate than NiP one. NiP/SiC500 has bigger passive range (ΔE) than the others which can be related to the higher coverage of the NiP matrix by inert particles. However, the difference between the coatings are negligible.

Literature reports different results related to the effect of ceramic particles on corrosion resistance of the coatings. Shakoor et al. [5] showed that addition of $Al_2O_3$ particles by electrodeposition to NiB coatings, increases the corrosion resistance of the coatings which was attributed to the reduction of active surface area of the matrix. Whereas, Araghi et al. [21] observed the reduction of corrosion resistance by addition $B_4C$ to NiP coating by electroless deposition. According to these studies and the current study, it seems that not only the particles and their sizes but also the matrix as well as the deposition method can affect the corrosion resistance of the coatings.

The breakdown potential around 300 mV (Fig. 8a) is due to trans-passivation. It has been assumed that nickel is preferentially dissolved at open circuit potential and left an enriched surface of phosphorus on the coatings [49,50].

Heat-treated coatings exhibit different polarization behavior as seen in Fig. 8b. They demonstrate an active anodic polarization although the corrosion current is smaller than that of as-plated coatings during the initial stages of the polarization. The shift of anodic polarization of heat-treated coatings to lower corrosion current density is attributed to the thermal oxide layer that was grown on the surface during the heat-treatment in air. Indeed, the oxide layer can decrease the corrosion current of the coatings while the corrosion resistance of these coatings suffers by cracking due to crystallization and precipitations which expose the steel substrate to the electrolyte. To confirm the effect of the oxide layer, the coatings were also heat-treated in an Ar atmosphere and their polarization curves were plotted in Fig. 8c. Here, all coatings have

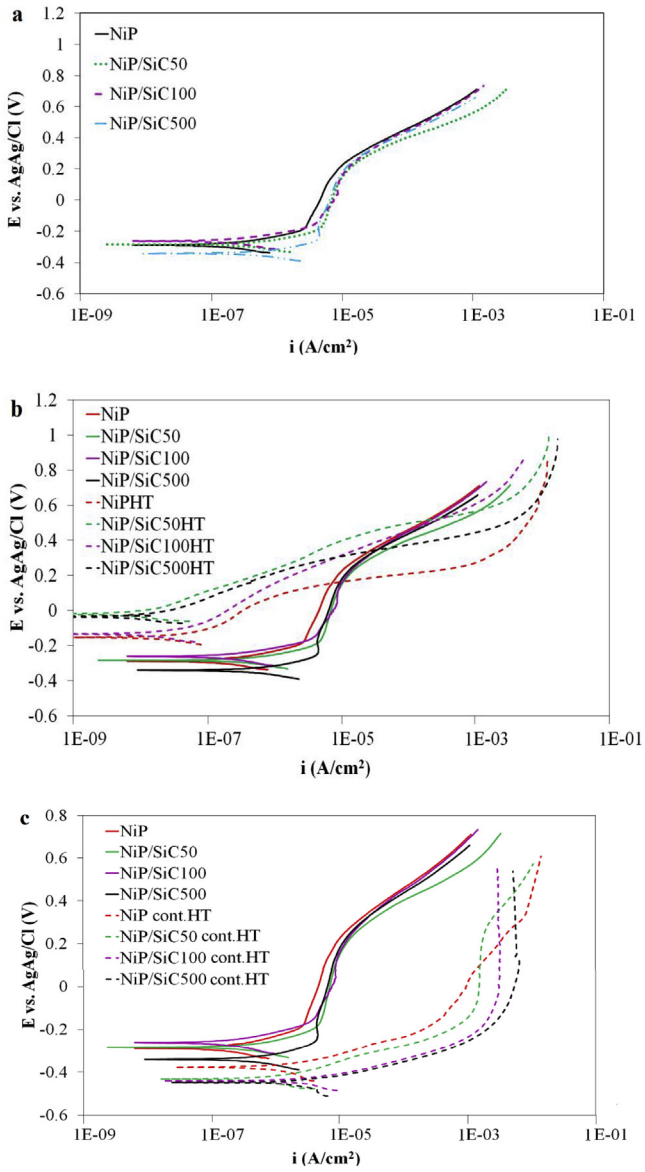


**Fig. 8.** Polarization curves of (a) as-plated and (b) heat-treated NiP and composite coatings in air, (c) heat-treated NiP and composite coatings in Ar atmosphere.

**Table 2**
$E_{corr}$ and $I_{corr}$ of as-plated NiP and composite coatings in 3.5% NaCl.

| Coatings | NiP | NiP/SiC50 | NiP/SiC100 | NiP/SiC500 |
|---|---|---|---|---|
| ΔE (V) | 0.40 | 0.43 | 0.39 | 0.49 |
| $E_{corr}$ (V) | −0.31 | −0.28 | −0.24 | −0.34 |
| $I_{corr}$ (A/cm$^2$) | $1.8 \times 10^{-6}$ | $6.4 \times 10^{-6}$ | $3.4 \times 10^{-6}$ | $7.2 \times 10^{-7}$ |
| $\beta_a$ (V/dec) | 0.77 | 0.58 | 0.78 | 0.67 |

active anodic polarization behavior with higher corrosion current density with respect to the as-plated ones. Furthermore, all samples show a lower corrosion potential proving the presence of microcracks exposing the substrate to the electrolyte. In addition, the color of heat-treated coatings in air was changed to blue while for the heat-treated samples in Ar, the color of the coatings was remained gray which is another evidence of formation thermal oxide layer on heat-treated samples in air.

After heat-treatment in the air, NiP/SiC50 and 500 have more noble $E_{corr}$ than NiP and NiP/SiC100 and as a result higher anodic polarization current was obtained in NiP and NiP/SiC100. While, in case of controlled atmosphere, $E_{corr}$ was the same for all composite coatings and a bit more negative than NiP and the anodic polarization current increased by addition SiC particles as well as increasing the size of the particles.

Ceramic particles are inert materials; therefore, when they are embedded in the metallic matrix, they will not directly contribute to corrosion properties. Nevertheless, during matrix crystallization, they can create defects in the coating by reducing the coherency and consistency of the matrix and their interface with the matrix is a susceptible area for corrosion or can hinder a resistant passive layer formation. In this study, NiP coatings are amorphous coatings that exhibits passive behavior and addition of ceramic particles did not affect noticeably the corrosion behavior. Although bigger SiC particles (SiC500) results in bigger passive range which can be related to the more coverage of NiP matrix. By heat-treatment in air there is no relation between the size of the particles and $E_{corr}$ or corrosion current which can be related to the formation of oxide layer that interferes in the corrosion behavior. While heat-treatment in Ar demonstrates that with increasing the size of SiC particles, higher anodic current is achieved which can be attributed to the formation of more microcrack by bigger SiC particles.

In this study, corrosion rate of NiP and composite coatings in as-plated condition in 3.5% NaCl varied between $10^{-6}$ to $10^{-7}$ A/cm$^2$. Corrosion rate of hard chromium one is around $10^{-6}$ to $10^{-8}$ A/cm$^2$ as Saghi Beyragh et al. [47] and Serres et al. [51] obtained. Therefore, as-plated NiP and composite coatings demonstrate similar corrosion resistance but less microhardness than hard Cr one while the heat-treated NiP and composite coatings have similar microhardness but less corrosion resistance than hard Cr one.

## 4. Conclusions

In this study, the effect of SiC (50, 100 and 500 nm) particles as well as heat-treatment on the properties of NiP coatings have been studied and the following results were concluded.

1. Ceramic particles and their size affected the coatings morphology, nano particles reduced the size of nodularity of NiP coatings, while sub-micron particles decreased the nodularity.
2. Heat-treatment had more influence on increasing the microhardness of the coatings than addition of the ceramic particles. Nevertheless, the particles had an extensive hardening effect in combination with heat-treatment.
3. Nanometer SiC particles deposited in less vol% but higher density than submicron ones resulted in comparable microhardness value.
4. Addition of ceramic particles did not have any significant effect on electrochemical behavior of the coatings. By heat-treatment the protective ability of the coatings was reduced due to the formation of microcracks.

## Acknowledgments

The authors acknowledge the financial support of European Union's for PROCETS project (Horizon 2020 research and innovation program under grant agreement No 686135).

The experimental support regarding to the bath recipe of the present work by Prof. Luca Magagnin from University of Politecnico di Milano is highly acknowledged.

## References

[1] A. Martínez-hernández, F. Manríquez-guerrero, J. Torres, R. Ortega,

J.D.J. Pérez-bueno, Y. Meas, G. Trejo, A. Méndez-albores, Electrodeposition of Ni-p/SiC Composite Films with High Hardness, Electrodeposition of Composite Materials, Chapter 7, INTECH Publisher, 2016, pp. 123–146.
[2] L. Wang, Y. Gao, Q. Xue, H. Liu, T. Xu, A novel electrodeposited Ni-P gradient deposit for replacement of conventional hard chromium, Surf. Coatings Technol. 200 (2006) 3719–3726.
[3] M.H. Allahyarzadeh, M. Aliofkhazraei, A.R.S. Rouhaghdam, V. Torabinejad, Electrochemical tailoring of ternary Ni-W-Co($Al_2O_3$) nanocomposite using pulse reverse technique, J. Alloys Compd. 705 (2017) 788–800.
[4] M.H. Allahyarzadeh, M. Aliofkhazraei, A.R. Rezvanian, V. Torabinejad, A.R.S. Rouhaghdam, Ni-W electrodeposited coatings: characterization, properties and applications, Surf. Coatings Technol. 307 (2017) 978–1010.
[5] R.A. Shakoor, R. Kahraman, U. Waware, Y. Wang, W. Gao, Properties of electrodeposited Ni – B – $Al_2O_3$ composite coatings, J. Mater. 64 (2014) 127–135.
[6] E. Valova, Interface with substrates of high-phosphorus electroless NiP and NiCuP deposited from nonammonia alkaline solutions, J. Electrochem. Soc. 143 (1996) 2804.
[7] L. Wu, Z. Yang, G. Qin, Kinetic study of a novel electroless NiP deposition on AZ91D magnesium alloy using nickel hypophosphite as the metal salt, J. Alloys Compd. 694 (2017) 1133–1139.
[8] J. Sudagar, J. Lian, W. Sha, Electroless nickel, alloy, composite and nano coatings - a critical review, J. Alloys Compd. 571 (2013) 183–204.
[9] M. Buchtík, P. Kosár, J. Wasserbauer, J. Tkacz, P. Doležal, Characterization of electroless Ni–P coating prepared on a wrought ZE10 magnesium alloy, Coatings 8 (2018) 96.
[10] I. Apachitei, F.D. Tichelaar, J. Duszczyk, L. Katgerman, The effect of heat treatment on the structure and abrasive wear resistance of autocatalytic NiP and NiP – SiC coatings, Surf. Coatings Technol. 149 (2002) 263–278.
[11] S. Karthikeyan, L. Vijayaraghavan, S. Madhavan, A. Almeida, Study on the mechanical properties of heat-treated electroless NiP coatings reinforced with $Al_2O_3$ nano particles, Metall. Mater. Trans. A Phys. Metall. Mater. Sci. 47 (2016) 2223–2231.
[12] H. Luo, M. Leitch, Y. Behnamian, Y. Ma, H. Zeng, J. Luo, Development of electroless Ni–P/nano-WC composite coatings and investigation on its properties, Surf. Coatings Technol. 277 (2015) 99–106.
[13] W.E.G. Hansal, G. Sandulache, R. Mann, P. Leisner, Pulse-electrodeposited NiP – SiC composite coatings, Electrochim. Acta 114 (2013) 851–858.
[14] O. Berkh, A. Bodnevas, J. Zahavi, Properties of electrodeposited Ni-P-SiC composite coatings, Met. Finish. 94 (1996) 35–40.
[15] Q. Wang, M. Callisti, J. Greer, B. McKay, T.K. Milickovic, A. Zoikis-Karathanasis, I. Deligkiozi, T. Polcar, Effect of annealing temperature on microstructure, mechanical and tribological properties of nano-SiC reinforced Ni-P coatings, Wear 356–357 (2016) 86–93.
[16] U. Matik, Structural and wear properties of heat-treated electroless Ni-P alloy and Ni-P-$Si_3N_4$ composite coatings on iron based PM compacts, Surf. Coatings Technol. 302 (2016) 528–534.
[17] C.F. Malfatti, J.Z. Ferreira, C.B. Santos, NiP/SiC composite coatings: the effects of particles on the electrochemical behaviour, Corrosion Sci. 47 (2005) 567–580.
[18] I. Garcia, Improved corrosion resistance through microstructural modifications induced by codepositing SiC-particles with electrolytic nickel, Corrosion Sci. 45 (2003) 1173–1189.
[19] C. Zanella, M. Lekka, P.L. Bonora, Influence of the particle size on the mechanical and electrochemical behaviour of micro and nano-nickel matrix composite coatings, J. Appl. Electrochem. 39 (2009) 31–38.
[20] I.R. Aslanyan, J. Bonino, J. Celis, Effect of reinforcing submicron SiC particles on the wear of electrolytic NiP coatings Part 1 . Uni-directional sliding, Surf. Coatings Technol. 200 (2006) 2909–2916.
[21] A. Araghi, M.H. Paydar, Electroless deposition of Ni-P-$B_4C$ composite coating on AZ91D magnesium alloy and investigation on its wear and corrosion resistance, Mater. Des. 31 (2010) 3095–3099.
[22] Z. Shafiee, M.E. Bahrololoom, B. Hashemi, Electrodeposition of nanocrystalline Ni/Ni – $Al_2O_3$ nanocomposite modulated multilayer coatings, Mater. Des. 108 (2016) 19–26.
[23] M. Allahyarzadeh, M. Aliofkhazraei, A.S. Rouhaghdam, V. Torabinejad, Electrodeposition of multilayer Ni–W and Ni–W–alumina nanocomposite coatings, Surf. Eng. 33 (2017) 327–336.
[24] M.H. Allahyarzadeh, M. Aliofkhazraei, A.R. Sabour Rouhaghdam, V. Torabinejad, Electrodeposition of Ni–W–$Al_2O_3$ nanocomposite coating with functionally graded microstructure, J. Alloys Compd. 666 (2016) 217–226.
[25] M.H. Allahyarzadeh, M. Aliofkhazraei, A.R.S. Rouhaghdam, V. Torabinejad, Gradient electrodeposition of Ni-Cu-W ( alumina ) nanocomposite coating, Mater. Des. 107 (2016) 74–81.
[26] H. Li, Y. He, T. He, D. Qing, F. Luo, Y. Fan, X. Chen, Ni-W/BN ( h ) electrodeposited nanocomposite coating with functionally graded microstructure, J. Alloys Compd. 704 (2017) 32–43.
[27] E. Beltowska-lehman, P. Indyka, A. Bigos, M.J. Szczerba, M. Kot, Ni – W/$ZrO_2$ nanocomposites obtained by ultrasonic DC electrodeposition, Mater. Des. 80 (2015) 1–11.
[28] A. Hadipour, S.M. Monirvaghefi, M.E. Bahrololoom, Electroless deposition of graded Ni–P coatings, Surf. Eng. 31 (2015) 399–405.
[29] M. Lekka, A. Lanzutti, C. Zanella, G. Zendron, L. Fedrizzi, P.L. Bonora, Resistance to localized corrosion of pure Ni , micro- and nano-SiC composite electrodeposits, Pure Appl. Chem. 83 (2011) 295–308.
[30] R. Bernasconi, F. Allievi, H. Sadeghi, L. Magagnin, The International Journal of Surface Engineering and Coatings Codeposition of nickel – phosphorus alloys reinforced with boron carbide microparticles: direct and pulse plating Codeposition of nickel – phosphorus alloys reinforced with boron carbide micro, J. Surf. Eng. Coat. 2967 (2017) 52–59.
[31] K. Dhanapal, V. Narayanan, A. Stephen, Effect of phosphorus on magnetic property of Ni-P alloy synthesized using pulsed electrodeposition, Mater. Chem. Phys. 166 (2015) 153–159.
[32] M. Sarret, C. Müller, A. Amell, Electroless NiP micro- and nano-composite coatings, Surf. Coatings Technol. 201 (2006) 389–395.
[33] A.M. Pillai, A. Rajendra, A.K. Sharma, Electrodeposited nickel – phosphorous ( Ni – P ) alloy coating: an in-depth study of its preparation, properties, and structural transitions, J. Coating Technol. Res. 9 (2012) 785–797.
[34] S.S. Djokic, Electrodeposition of amorphous alloys based on the iron group of metals, J. Electrochem. Soc. 146 (1999) 1824–1828.
[35] Z. Guo, K.G. Keong, W. Sha, Crystallisation and phase transformation behaviour of electroless nickel phosphorus platings during continuous heating, J. Alloys Compd. 358 (2003) 112–119.
[36] R. Taheri, Evaluation of Electroless Nickel-phosphorus (EN) Coatings, PhD Thesis, University of Saskatchewan, 2003.
[37] J.N. Balaraju, K.S. Rajam, Electroless deposition and characterization of high phosphorus, Int. J. Electrochem. Sci. 2 (2007) 747–761.
[38] G. Jiaqiang, W. Yating, L. Lei, H. Wenbin, Crystallization behavior of nanometer-sized Al 2 O 3 composite coatings prepared by electroless deposition, Mater. Lett. 59 (2005) 391–394.
[39] J.N. Balaraju, K.S. Rajam, Preparation and characterization of autocatalytic low phosphorus nickel coatings containing submicron silicon nitride particles, J. Alloys Compd. 459 (2008) 311–319.
[40] M. Chou, M. Ger, S. Ke, Y. Huang, S. Wu, The Ni – P – SiC composite produced by electro-codeposition, Mater. Chem. Phys. 92 (2005) 146–151.
[41] I. Garcia, J. Fransaer, J.P. Celis, Electrodeposition and sliding wear resistance of nickel composite coatings containing micron and submicron SiC particles, Surf. Coatings Technol. 148 (2001) 171–178.
[42] N.P. Wasekar, S.M. Latha, M. Ramakrishna, D.S. Rao, G. Sundararajan, Pulsed electrodeposition and mechanical properties of Ni-W/SiC nano-composite coatings, Mater. Des. 112 (2016) 140–150.
[43] Richard W. Hertzberg, Richard P. Vinci, Jason L. Hertzberg, Deformation and Fracture Mechanics of Engineering Materials, fifth ed., Wiley, 2012.
[44] L. Chang, P.W. Kao, C.H. Chen, Strengthening mechanisms in electrodeposited Ni-P alloys with nanocrystalline grains, Scr. Mater. 56 (2007) 713–716.
[45] A.F. Zimmerman, D.G. Clark, K.T. Aust, U. Erb, Pulse electrodeposition of Ni–SiC nanocomposite, Mater. Lett. 52 (2002) 85–90.
[46] A.S. El-Amoush, A. Abu-Rob, H. Edwan, K. Atrash, M. Igab, Tribological properties of hard chromium coated 1010 mild steel under different sliding distances, Solid State Sci. 13 (2011) 529–533.
[47] M.R. Saghi Beyragh, A. Sh. Khameneh, S. Norouzi, A comparative research on corrosion behavior of a standard, crack-free and duplex hard chromium coatings, Surf. Coatings Technol. 205 (2010) 2605–2610.
[48] M.H. Sohi, F. Ghadami, Tribology International Comparative tribological study of air plasma sprayed WC – 12 % Co coating versus conventional hard chromium electrodeposit, Tribiol. Int. 43 (2010) 882–886.
[49] C. Ma, F. Wu, Y. Ning, F. Xia, Y. Liu, Effect of heat treatment on structures and corrosion characteristics of electroless Ni – P – SiC nanocomposite coatings, Ceram. Int. 40 (2014) 9279–9284.
[50] Y.F. Shen, W.Y. Xue, Z.Y. Liu, L. Zuo, Nanoscratching deformation and fracture toughness of electroless Ni-P coatings, Surf. Coatings Technol. 205 (2010) 632–640.
[51] N. Serres, F. Hlawka, S. Costil, C. Langlade, F. MacHi, Corrosion properties of in situ laser remelted NiCrBSi coatings comparison with hard chromium coatings, J. Mater. Process. Technol. 211 (2011) 133–140.